

Steerable frequency-invariant beamforming for arbitrary arrays

Lucas C. Parra^{a)}

Biomedical Engineering Department, City College of New York, New York 10031

(Received 9 September 2005; revised 27 March 2006; accepted 28 March 2006)

Frequency-invariant beamforming aims to parameterize array filter coefficients such that the spectral and spatial response profiles of the array can be adjusted independently. Solutions to this problem have been presented for specific sensor configurations often requiring a larger number of sensors. However, in practical applications, the number and location of sensors are often restricted. This paper proposes to find an optimal linear basis transformation that decouples the frequency response from the spatial response. A least-squares optimal basis transform can be computed numerically for arbitrary sensor configurations, for which typically no exact analytical solutions are available. This transform can be further combined with a spherical harmonics basis resulting in readily steerable broadband beams. This solution to broadband beamforming effectively decouples the array geometry from the steering geometry. Furthermore, for frequency-invariant beams, this approach results in a significant reduction in the number of beam-design parameters. Here, the method is demonstrated for an optimal design of far-field response for an irregular linear array with as few as three sensors. © 2006 Acoustical Society of America. [DOI: 10.1121/1.2197606]

PACS number(s): 43.60.Fg [EJS]

Pages: 3839–3847

I. INTRODUCTION

An array of spatially distributed sensors can be made selective in space and frequency by filtering and summing the output of multiple sensors. For a fixed geometry, the spectro-spatial response profile is determined by the filter coefficients. Changing a given coefficient will typically affect both the frequency as well as the spatial response profile. This spectro-spatial coupling complicates broadband filter design as well as adaptive beamforming algorithms. The goal of this work is to find a parameterization of the filter coefficients that decouples the spatial selectivity from the frequency selectivity for arbitrary array configurations. Once decoupled, a frequency-invariant response is obtained by choosing the same coefficients for multiple frequencies. This simplifies broadband beamforming as the frequency response and the spatial profile can be adjusted independently.

Broadband and frequency-invariant beamforming has been addressed by Ward *et al.*,¹ covering far-field problems, and Abhayapala *et al.*² and Kennedy *et al.*³ for near-field problems. Their approach is based on the spatial Fourier transform of a continuous aperture. In practical implementations, the aperture needs to be sampled with a discrete number of sensors. This leads to specific array configurations typically with a large number of sensors on a linear or rectangular lattice.^{2,4,5} More recent work presents analytic inversion methods for linear,⁶ cylindrical,⁷ and spherical arrays.⁸ Although these array configurations may be optimal in terms of frequency invariance, reduced aliasing, or spatial resolution, they may not be practical in some applications. In particular, speech acquisition with embedded microphones requires broadband arrays often with a very small number of microphones (two to five) in a constrained spatial arrange-

ment. This paper presents a numerical approach to construct an optimal frequency-invariant response for an arbitrarily chosen array configuration.

Following previous work,⁸ the resulting frequency-invariant response is made steerable by combining it with the spherical harmonics decomposition of the beam pattern.^{2,9} The required coefficients for rotating spherical harmonics are given by the Wigner rotation matrix.¹⁰ A numerical approach related to the present method has been considered in the context of near-field design but has not been fully developed.³ A related technique has been presented for arbitrarily placed sensors on a sphere but without addressing frequency invariance.¹¹

The paper is organized as follows: Secs. II and III introduce the notation and define the goal of frequency-invariant beamforming. Sections IV and V present existing solutions based on analytic expansions of plane waves and the corresponding inversion formulas. The numerical least-squares approach proposed in this work is presented in Sec. VI. Beam steering is discussed in Sec. VII giving some special considerations to the linear array. Section VIII discusses sensor noise and the resulting regularization of the least-squares solution. Section IX explains how the proposed basis transformation can be used to make existing adaptive beamforming algorithms frequency invariant. Finally, examples are presented using data-independent beam design for a linear array. The paper closes with a discussion on how the proposed method can be applied to other array configurations, directional sensors, and near-field beam design. To better follow the main argument, the reader may skip Secs. IV, V, VII A, and VIII in a first reading.

II. ARRAY RESPONSE

This section defines some terminology commonly used with sensor arrays and beam forming. Denote the signal sampled by the n th sensor at time t as $x_n(t)$. A beamformer

^{a)}Electronic mail: parra@ccny.cuny.edu

convolves the N sensor signals with the corresponding filter coefficients $c_n(t)$ and sums the result to generate an array output signal:

$$y(t) = \sum_{n=1}^N c_n(t) * x_n(t). \quad (1)$$

The convolution is denoted here with the symbol $*$.

For far-field design, it is customary to discuss the effect of this processing by considering the signals produced by a planar wave impinging on the sensors. Assume a steady-state plane wave with radial frequency ω traveling in direction $\Omega = (\vartheta, \varphi)$, where spherical angles ϑ and φ represent elevation and azimuth, respectively. Orientation and frequency can also be specified in Cartesian coordinates as a three-vector \mathbf{k} pointing in direction Ω with $k = \|\mathbf{k}\|$ characterizing the wavenumber $k = \omega/c$. Because of the simple linear relationship, the wavenumber k will also be referred to as “frequency” in this paper. The plane wave elicits, at location \mathbf{r}_n , a pressure signal:⁹

$$x_n(t) = e^{i(\mathbf{k} \cdot \mathbf{r}_n - \omega t)}, \quad (2)$$

with $i^2 = -1$. To obtain the angle-dependent frequency response, consider the temporal Fourier transform \mathcal{F} of this pressure signal:

$$x_n(\nu) = \mathcal{F}\{x_n(t)\} = 2\pi\delta(\nu - \omega)e^{i\mathbf{k} \cdot \mathbf{r}_n}. \quad (3)$$

This is the response of the sensors to the plane wave which defines the *sensor response* $g_n(\mathbf{k})$:

$$g_n(\mathbf{k}) = e^{i\mathbf{k} \cdot \mathbf{r}_n}. \quad (4)$$

The δ -function expresses the monochromatic nature of the plane wave, and is typically omitted to facilitate a more compact notation.⁹ Similarly, the Fourier transform of the resulting response of the filter and sum:

$$y(\nu) = \mathcal{F}\{y(t)\} = 2\pi\delta(\nu - \omega)f(\mathbf{k}), \quad (5)$$

leads to the definition of the *filter-array response* $f(\mathbf{k})$:

$$f(\mathbf{k}) = \sum_{n=1}^N c_n(k)g_n(\mathbf{k}). \quad (6)$$

III. FREQUENCY-INVARIANT BEAMFORMING

Now consider Eq. (6) with \mathbf{k} rewritten in terms of the *arrival direction* Ω and frequency k ,

$$f(k, \Omega) = \sum_{n=1}^N c_n(k)g_n(k, \Omega). \quad (7)$$

This equation can be seen as a parameterization of the filter-array response for each frequency k with coefficients $c_n(k)$, and basis functions $g_n(k, \Omega)$. Modifying coefficients $c_n(k)$ will affect the frequency and spatial response simultaneously because $g_n(k, \Omega)$ depends on both the frequency k and arrival direction Ω . The goal of *frequency-invariant beamforming* is to find a new parameterization for $c_n(k)$:

$$c_n(k) = \sum_{l=1}^L b_{nl}(k)\tilde{c}_l(k), \quad (8)$$

such that the basis transform $b_{nl}(k)$ converts the array response into a frequency-invariant array response,

$$\sum_{n=1}^N g_n(k, \Omega)b_{nl}(k) = \tilde{g}_l(\Omega). \quad (9)$$

The basis transform replaces the N sensors indexed by n by a new set of L *virtual* sensors indexed by l . These virtual sensors are now frequency invariant. This basis transform, in turn, factorizes the filter-array response, which is seen by combining Eqs. (7)–(9):

$$f(k, \Omega) = \sum_{l=1}^L \tilde{c}_l(k)\tilde{g}_l(\Omega). \quad (10)$$

By comparing Eq. (10) with Eq. (7), it becomes clear that modifying the new parameters $\tilde{c}_l(k)$ will affect the spatial response profile $f(k, \Omega)$ only at frequency k . In fact, the spatial response profile of the filter array is fully determined by coefficients $\tilde{c}_l(k)$. In particular, a frequency-invariant beamformer is obtained by choosing the same coefficients for all frequencies, $\tilde{c}_l(k) = \tilde{c}_l$.

The challenge of uncoupling the spatial from the spectral response lies in finding a basis transform $b_{nl}(k)$ that satisfies Eq. (9)—even if only approximately.

IV. ARRAY RESPONSE FOR VARIOUS GEOMETRIES

To understand existing analytic solutions to this problem, it will be useful to express the sensor response [Eq. (4)] in terms of the arrival direction Ω . The plane wave response of a sensor located at $\mathbf{r}_n = (r'_n, \Omega'_n)$ can be expanded^{10,9} as

$$g_n(k, \Omega) = 4\pi \sum_{l=0}^{\infty} i^l j_l(kr'_n) \sum_{m=-l}^l Y_l^m(\Omega) Y_l^{m*}(\Omega'_n), \quad (11)$$

where $j_l(kr)$ are spherical Bessel functions of the first kind, and $Y_l^m(\Omega)$ are spherical harmonics. The response of a spherical array is given by Eq. (11) with $r'_n = r'$. For a horizontally placed circular array with $\vartheta'_n = \pi/2$, and restricting to the horizon as arrival direction $\vartheta = \pi/2$, Eq. (11) becomes⁷

$$g_n(k, \varphi) = \sum_{l=-\infty}^{\infty} i^l J_l(kr') e^{il(\varphi - \varphi'_n)}, \quad (12)$$

where $J_l(kr)$ are Bessel functions of the first kind. In a vertically aligned linear array with $\vartheta'_n = 0$, Eq. (11) becomes independent of φ , and is therefore symmetric about the array axis:⁶

$$g_n(k, \Omega) = e^{-ikr'_n \cos \vartheta}. \quad (13)$$

V. ANALYTIC INVERSION APPROACHES

Let us now consider existing analytic solutions to the factorization problem (9). A general theory for continuous apertures has been proposed¹ with corresponding approximations for discrete arrays.^{1,5} Some specific array configura-

tions make use of elegant analytic inversion formulas, as in the case of spherical,⁸ hemispherical,¹² circular,^{13,7} linear,⁶ and rectangular⁴ arrays. Equations (11)–(13) were presented to give an indication of possible approaches. To give an idea of these methods, consider the case of a circular array. For a circular array, one may choose:

$$b_{nl}(k) = N^{-1} i^{-l} J_l^{-1}(kr) e^{il\varphi_n}. \quad (14)$$

Inserting Eqs. (14) and (12) into Eq. (9) will indeed give a frequency-invariant function of space, $\tilde{g}_l(\varphi) = e^{-il\varphi}$, assuming that the following orthogonality condition holds for any l, m :

$$\frac{1}{N} \sum_{n=1}^N e^{i(m-l)\varphi_n} = \delta_{ml}. \quad (15)$$

Unfortunately, this is only correct for $|l| < N$, and only if the N sensors are placed on an equidistant lattice along the circular array. As a result, Eq. (9) is only approximately correct. For circular, as well as spherical, arrays the approximation can only be improved with a larger number of sensors, while the lattice must be carefully arranged to match the analytic inversion formulas.^{13,8} The same is true for linear and rectangular arrays.^{1,5} In addition, for those configurations, the angular response profile at any given frequency only partially determines the required spatial Fourier basis coefficients.⁶ Arbitrary Fourier coefficients have to be chosen outside of the determined range, further compromising the accuracy of the approximations.

VI. LEAST-SQUARES SOLUTION

The goal of this work is to directly minimize the approximation error resulting from the restricted number of sensors, and to overcome the restrictions on sensor locations imposed by analytic inversions. The proposed solution is to invert Eq. (9) numerically. To this end, discretize the arrival directions with angles Ω_q , $q=1, \dots, Q$, and write Eq. (9) in matrix notation

$$\mathbf{G}(k)\mathbf{B}(k) = \tilde{\mathbf{G}}, \quad (16)$$

where $[\mathbf{G}(k)]_{qn} = g_n(k, \Omega_q)$, $[\mathbf{B}(k)]_{nl} = b_{nl}(k)$, and $[\tilde{\mathbf{G}}]_{ql} = \tilde{g}_l(\Omega_q)$. The new desired spatial basis vectors can be defined in the columns of $\tilde{\mathbf{G}}(k)$, while $\mathbf{G}(k)$ is determined by the array configuration. For each frequency, k , Eq. (16) specifies LQ conditions with LN unknowns. Typically, only a few sensors are available; yet one would like to parameterize the response for many different arrival directions. Therefore, with $Q > N$, the problem is overdetermined. The *least-squares* solution to this problem (i.e., the \mathbf{B} that will reproduce \mathbf{G} with the smallest square error) is computed with the pseudo-inverse, $\mathbf{G}^\dagger = (\mathbf{G}^H \mathbf{G})^{-1} \mathbf{G}^H$,

$$\mathbf{B}(k) = \mathbf{G}^\dagger(k) \tilde{\mathbf{G}}. \quad (17)$$

This requires that \mathbf{G} is of full rank—a condition that has to be verified in practice. Note that the discretization of the arrival directions is only used to compute the basis transform $b_{nl}(k)$. When applying the new basis, the arrival direction can take on any arbitrary values. For a given array geometry, the

basis transform is computed once for each frequency, k , and remains unaltered by subsequent beam design.

The accuracy of the proposed method depends on how well \mathbf{G} can be inverted, that is, how well can $\tilde{\mathbf{G}}$ be represented by \mathbf{B} : $\varepsilon = \|\mathbf{G}\mathbf{B} - \tilde{\mathbf{G}}\|^2 = \|\mathbf{G}\mathbf{G}^\dagger \tilde{\mathbf{G}} - \tilde{\mathbf{G}}\|^2$. This is the minimum attainable square error in satisfying the factorization condition (9) for a specific set of angles Ω_q . Any other basis transform is suboptimal (in the least-squares sense).

Uniform sampling of angles Ω gives equal weight to the optimality criteria ε . Nonuniform sampling will place a bigger weight on the areas in angular space that are sampled more densely. To avoid large errors for intermediate angles that have not been sampled, one should choose band-limited basis functions $\tilde{\mathbf{G}}$. Spherical harmonics represent such a basis and will be presented next.

VII. BEAM STEERING

Ideally, the new spatial basis, $\tilde{g}_l(\Omega)$, should be easily steerable. This means that the overall orientation of a beam can be rotated without changing its spatial profile, i.e., without changing coefficient $\tilde{c}_l(k)$. This implies that after rotation of the frame of reference, the basis can be expressed in terms of the same basis. The basis of spherical harmonics satisfies this property;

$$Y_l^m(\Omega') = \sum_{m=-l}^l D_{mm'}^l(\alpha, \beta, \gamma) Y_l^m(\Omega). \quad (18)$$

Ω and Ω' are the spherical angles before and after the rotation of the frame of reference. The rotation can be specified by the Euler angles α, β, γ , where γ is an initial spin about the original z axis, β changes its elevation, and α is a subsequent change in longitude. Explicit expressions for coefficients $D_{mm'}^l(\alpha, \beta, \gamma)$ were first given by Wigner^{10,14} and are variably referred to as Wigner D -functions or Wigner rotation matrix. Efficient algorithms are available to compute these coefficients from a conventional 3×3 rotation matrix given in Cartesian coordinates.¹⁵

An additional advantage of the spherical harmonics is their uniform resolution.¹⁶ Equation (18) states that any rotated version of the spherical harmonics of order L can be represented exactly by harmonics of, at most, order L . This implies that band-limited beam patterns, which do not oscillate faster than π/L , can be represented exactly with harmonics of at most order L .^{17,18}

Thanks to identity (18) the spherical harmonics are readily steerable and therefore are a natural choice for the new basis:⁸

$$\tilde{g}_{lm}(\Omega) = Y_l^m(\Omega). \quad (19)$$

The virtual sensors now require double index lm instead of just l . With the matrix notation adopted for Eq. (16), a pair lm indexes a column of matrix $\tilde{\mathbf{G}}$. Arranging the Wigner rotation coefficients as matrix $[\mathbf{D}(\alpha, \beta, \gamma)]_{lm, l', m'}$ = $D_{mm'}^l(\alpha, \beta, \gamma)$, the basis is then rotated with

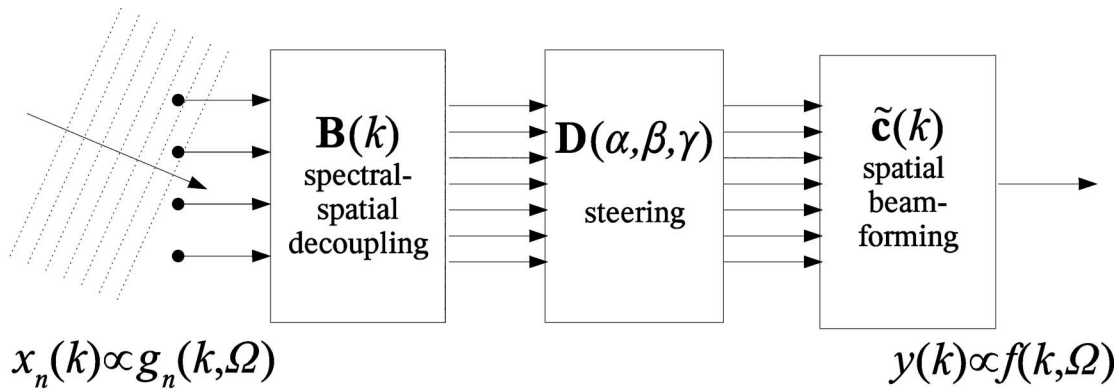


FIG. 1. Signal flow diagram.

$$\tilde{\mathbf{G}}' = \tilde{\mathbf{G}}\mathbf{D}(\alpha, \beta, \gamma), \quad (20)$$

and the basis transform that includes an arbitrary rotation is given by

$$\mathbf{B}'(k, \alpha, \beta, \gamma) = \mathbf{B}(k)\mathbf{D}(\alpha, \beta, \gamma). \quad (21)$$

To summarize the overall design structure, let us combine the previous equations in a compact form. The response of the array is now given by

$$f(k, \Omega) = \mathbf{g}(k, \Omega)\mathbf{B}(k)\mathbf{D}(\alpha, \beta, \gamma)\tilde{\mathbf{c}}(k). \quad (22)$$

The corresponding signal-flow diagram is shown in Fig. 1. Vector $\mathbf{g}(k, \Omega)$ is the response of the N sensors to a plane wave. $\mathbf{B}(k)$ uncouples the spatial response from the spectral response. $\mathbf{D}(\alpha, \beta, \gamma)$ steers the spatial response into an arbitrary direction; and $\tilde{\mathbf{c}}(k)$ defines its spatial profile for each frequency separately. Choosing the same coefficients $\tilde{\mathbf{c}}(k)$ for all frequencies yields an array response that is frequency invariant.

This structure uncouples the steering geometry from that of the array geometry. In previous approaches, the ability to steer seemed inevitably linked to the choice of array architecture and the corresponding analytic inversion formulas. The problem of steering the array has also been uncoupled from that of choosing its spatial profile, and finally, the design of the frequency response has been separated from that of the spatial response.

A. Steering in a linear array

For the special case of a linear array, the situation is complicated by the lack of full control over the two-dimensional beam pattern. In a vertical linear array, one can specify the response profile only in elevation ϑ . Rotating an axis-symmetric shape in elevation by β violates the axial symmetry around the z axis. Therefore, one cannot rotate a beam pattern by angle β and at the same time preserve symmetry in φ . As a result, there is no basis in ϑ that is isomorphic with respect to a shift. However, one can aim to find a transformation that approximately preserves a spatial profile defined in $\vartheta \in [0, \pi]$. One may choose, for instance, the Legendre basis and expand its shifted version in the same basis function set;

$$P_{l'}(\cos \vartheta') \approx \sum_{l=0}^L D_{ll'}(\beta) P_l(\cos \vartheta), \quad (23)$$

$$D_{ll'}(\beta) = \frac{2l+1}{2} \int_0^\pi P_{l'}(\cos(\vartheta - \beta)) P_l(\cos \vartheta) d\cos \vartheta, \quad (24)$$

which defines a basis rotation or shift analogous to Eq. (18). The approximation results from the truncation of the sum at $L < \infty$. An optimal choice of basis would minimize this approximation error, implying that a shift of the basis can be expressed accurately within the same order ($l \leq L$). Therefore, in an ideal basis the shift matrix, $[\mathbf{D}(\beta)]_{ll'} = D_{ll'}(\beta)$, will have triangular structure such as in the case of spherical harmonics.¹⁶ Figure 2 shows that the shift matrix $\mathbf{D}(\beta)$ for the Legendre basis is, in fact, approximately triangular resulting in small truncation errors. Therefore, for the linear array we suggest to use,

$$\tilde{g}_l(\vartheta) = P_l(\cos \vartheta). \quad (25)$$

Using the appropriate definitions for matrix $\mathbf{D}(\beta)$ based on Eq. (24), one can write the corresponding equations for this *approximate shift* of the beam pattern as in Eqs. (20) and (21).

In principle, there should be a closed-form solution to integral (24). However, in practice, it may be more efficient to evaluate the integral once (perhaps numerically) for each desired shift angle β , and store the L^2 coefficients for later use. To evaluate the Legendre coefficients of a general function, $f(z)$, numerically one may discretize the angle with Q samples, $z_q = \cos \vartheta_q$, and convert the integral into a discrete sum. This can be expressed efficiently in matrix-vector notation by defining matrix $[\mathbf{P}]_{ql} = P_l(z_q)$, and vector $[\mathbf{f}]_q = f(z_q)$. The Legendre coefficient for function $f(z)$ arranged as vector $[\tilde{\mathbf{c}}]_l = \tilde{c}_l$ are computed with

$$\tilde{\mathbf{c}} = \mathbf{P}^\dagger \mathbf{f}, \quad (26)$$

where the pseudo-inverse \mathbf{P}^\dagger implements the integration sum and proper quadrature weights for any sampling of ϑ .¹⁹ Transformation (26) is inverted in approximation with

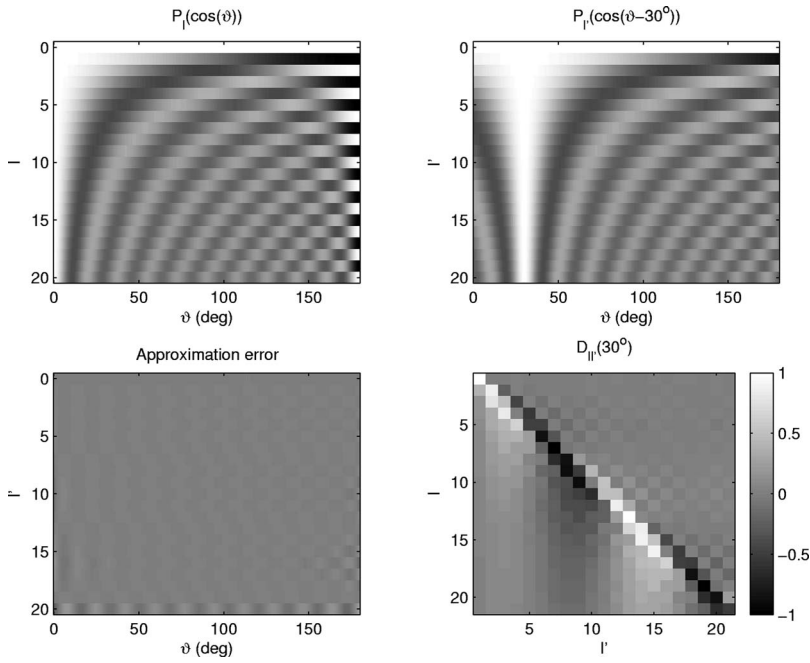


FIG. 2. Legendre basis functions and their rotations. Top two panels show Legendre basis functions as intensity images up to order $L=20$. Left and right panels represent $P_l(\vartheta)$ and $P_l(\vartheta-\beta)$. This example is for a rotation angle $\beta=30^\circ$. Bottom left panel shows the approximation error in Eq. (23) due to truncation at $L=20$. Bottom right panel shows the corresponding matrix $D_{ll'}$ as defined in Eq. (24). All four panels use the same intensity gray scale.

$$\mathbf{f} \approx \mathbf{P}\tilde{\mathbf{c}}. \quad (27)$$

As with any pseudo-inverse, the approximation is exact if $\dim(\mathbf{f})=\dim(\tilde{\mathbf{c}})$, while the square error is minimized for $\dim(\mathbf{f})>\dim(\tilde{\mathbf{c}})$. With this notation, the shift matrix $\mathbf{D}(\beta)$ in Eq. (24) is,

$$\mathbf{D}(\beta) = \mathbf{P}^\dagger \mathbf{P}'(\beta), \quad (28)$$

where matrix \mathbf{P}' captures the L Legendre polynomials evaluated at Q cosines shifted by β : $[\mathbf{P}'(\beta)]_{ql'} = P_{l'}(\cos(\vartheta_q - \beta))$.

VIII. EFFECTIVE BEAM CONTROL, MEASUREMENT NOISE, AND REGULARIZATION

When computing the basis \mathbf{B} with Eq. (17), it was required that matrix \mathbf{G} be of full rank. However, in practice, the matrix $\mathbf{G}^H(k)\mathbf{G}(k)$ is ill conditioned for the lowest frequencies and, therefore, cannot be accurately inverted when computing the pseudo-inverse $\mathbf{G}^\dagger(k)$. This is to be expected for very low frequencies with a large wavelength since a limited aperture prevents effective spatial resolution. Similarly, for high frequencies, the finite spacing of sensors generates aliasing side lobes, once again leading to a noninvertible $\mathbf{G}^H(k)\mathbf{G}(k)$ (recall the goal of using only a small number of sensors). This limitation is inherent to *any* beamforming design and is typically resolved by restricting the frequency band of operation or carefully choosing sensor spacing and array aperture. In the present numerical inversion approach, the instability leads to rather large gains which may arbitrarily magnify sensor noise. This section shows how this problem can be resolved by considering the effect of measurement noise.

Assume zero-mean wide-sense stationary additive sensor noise $w_n(t)$ with power spectrum $\sigma^2(k)$. The sensor signal in response to a plane wave is now (in the frequency domain)

$$x_n(k) = g_n(k, \Omega) + w_n(k). \quad (29)$$

With the appropriate definition of matrix $[\mathbf{W}(k)]_{qn} = w_n(k)$, Eq. (16) now becomes

$$(\mathbf{G}(k) + \mathbf{W}(k))\mathbf{B}(k) = \tilde{\mathbf{G}}. \quad (30)$$

Note that the signal of the steady-state plane wave $\mathbf{G}(k)$ is deterministic, while the noise $\mathbf{W}(k)$ is a random variable. To find the optimal basis, one now has to minimize the expected value over the random noise:

$$E[\|(\mathbf{G}(k) + \mathbf{W}(k))\mathbf{B}(k) - \tilde{\mathbf{G}}\|^2]. \quad (31)$$

For noise that is uncorrelated with the signal, this evaluates (omitting dependency on k) to the following trace:

$$\text{Tr}(\mathbf{B}^H(\mathbf{G}^H\mathbf{G} + E[\mathbf{W}^H\mathbf{W}])\mathbf{B} - \mathbf{B}^H\mathbf{G}^H\tilde{\mathbf{G}} - \tilde{\mathbf{G}}^H\mathbf{G}\mathbf{B}). \quad (32)$$

This criterion is minimized by

$$\mathbf{B} = (\mathbf{G}^H\mathbf{G} + \Sigma)^{-1}\mathbf{G}^H\tilde{\mathbf{G}}, \quad (33)$$

which, as usual, is obtained by setting the derivative with respect to \mathbf{B}^H equal to zero and solving for \mathbf{B} . If the noise is spatially uncorrelated and homogeneous in space, then the $N \times N$ matrix $\Sigma(k) = E[\mathbf{W}(k)^H\mathbf{W}(k)]$ is diagonal with powers $\sigma_n^2(k)$ on the diagonal. This result is the conventional regularization of the pseudo-inverse. The examples presented in Sec. XI will use this regularization.

IX. APPLICATION TO ADAPTIVE BEAMFORMING DESIGN

The time domain output $y(t)$ of the filter array in response to sensor readings $x_n(t)$ is given by the convolution and sum:

$$y(t) = \sum_{n=1}^N c_n(t) * x_n(t) = \sum_{l=1}^L \tilde{c}_l(t) * \tilde{x}_l(t). \quad (34)$$

The second equality here results from Eq. (8) and the following definition of the *frequency-invariant virtual sensor* readings:

$$\tilde{x}_l(t) = \sum_{n=1}^N b_{nl}(t) * x_n(t). \quad (35)$$

This suggests that adaptive algorithms, that are driven by the sensor observations, can be applied to the signals of the newly defined frequency-invariant virtual sensors. Instead of optimizing filter parameters, $c_n(k)$, based on sensor readings, $x_n(t)$, the adaptive algorithm now adapts parameters $\tilde{c}_l(k)$ based on virtual sensor readings, $\tilde{x}_l(t)$. All known adaptive beamforming algorithms, such as generalized side-lobe canceling, blind source separation, and others are, therefore, immediately applicable without further modification.

To find an optimal frequency-invariant response, the adaptive algorithm will now optimize the parameters \tilde{c}_l . If the algorithm is based on a gradient of some cost function, $J(\{\tilde{c}_l(k)\})$, with a set of frequency dependent parameters, $\{\tilde{c}_l(k)\}$, the frequency-invariant gradient is then simply the original gradient summed over all frequencies

$$\frac{\partial J}{\partial \tilde{c}_l} = \sum_k \frac{\partial J}{\partial \tilde{c}_l(k)}. \quad (36)$$

Note that this has the potential to significantly reduce the number of free parameters as the same coefficients are used for all frequencies. For most adaptive algorithms, this will result in significant improvements in convergence speed as well as estimation accuracy. This advantage is in addition to the potential advantage of a frequency-invariant response.

X. APPLICATION TO IRREGULAR LINEAR ARRAY WITH LEAST-SQUARES BEAM DESIGN

The proposed method was implemented for a linear array of omnidirectional sensors and Legendre polynomials as the beamforming basis, i.e., Eqs. (13) and (25). Notice that Eq. (13) does not require equidistant sensor placement. The least-squares solution given by Eq. (17) is used to compute the basis transform. Choosing Legendre polynomials, as in Eq. (25), as the frequency-invariant virtual array response in Eq. (17) means that

$$\tilde{\mathbf{G}} = \mathbf{P}. \quad (37)$$

The effectiveness of the resulting basis is demonstrated by estimating parameters $\tilde{\mathbf{c}}$ that optimally reproduce a desired beam pattern. To this end, one could use a variety of beam design methods.²⁰ A simple data-independent method is the least-squares beamformer, which will be used here. Assume the prescribed response is specified as a vector \mathbf{f} with coefficients f_d , each of which represents the desired response for angles θ_d , $d=1, \dots, D$. The response of the array at those angles can be written in matrix notation as

$$\mathbf{f} = \mathbf{G}(\boldsymbol{\theta})\mathbf{B}\tilde{\mathbf{c}}, \quad (38)$$

where the coefficients of matrix $\mathbf{G}(\boldsymbol{\theta})$ are given by $[\mathbf{G}]_{dn} = g_n(\theta_d)$ specifying the response of the n th sensor for the desired angle θ_d . The goal is to find the coefficient $\tilde{\mathbf{c}}$ that

reproduces the desired response \mathbf{f} . Equation (38) does not include rotation. Instead, rotation is introduced after determining the optimal coefficients for a desired response. With N sensors, one can satisfy, at most, N conditions on the response. A larger number of conditions can only be satisfied approximately. The coefficients that reproduce \mathbf{f} with the least-squares error are given by

$$\tilde{\mathbf{c}} = (\mathbf{G}(\boldsymbol{\theta})\mathbf{B})^\dagger \mathbf{f}. \quad (39)$$

Without going into detail, one should note that it is also useful to regularize this inverse, as in Eq. (33).

The Legendre basis uses L basis coefficients and can be rotated without having to recompute coefficients. One can compare this with the coefficient obtained in a *naive* frequency-invariant basis with $[\tilde{\mathbf{G}}]_{qm} = \delta_{qm}$ in Eq. (17). This basis requires Q coefficients, which is typically significantly larger than L , and the coefficients have to be recomputed when the response is to be rotated. For this “naive” basis, Eq. (39), simplifies to

$$\tilde{\mathbf{c}} = (\mathbf{G}(\boldsymbol{\theta})\mathbf{G}^\dagger)^\dagger \mathbf{f}. \quad (40)$$

In Eqs. (38)–(40), the dependence on frequency was omitted for simplicity. The optimal parameters for each frequency are computed with Eq. (39) or (40). For a frequency invariant basis, one should use the same coefficients for all frequency bands. One option is to use the coefficients computed with Eq. (40) averaged across frequencies, $\tilde{\mathbf{c}} = 1/T \sum_k \tilde{\mathbf{c}}(k)$. Though suboptimal, this approach is not only simpler but in practice shows also better error behavior compared to the “optimal” solution, which would require combining all frequencies prior to computing the pseudo-inverses in Eq. (39) or (40). Simulations show that this averaging of coefficients across frequencies results in more evenly distributed deviations from the desired solutions as compared to the globally optimal solution.

Note that even after regularization, effective beam design is not possible at frequencies for which $\mathbf{G}^H\mathbf{G}$ is not invertible. One measure for the instability of the inverse (or rank deficiency of \mathbf{G}) is the condition number. One can use the condition number as a criterion to exclude frequency bands when computing the average $\tilde{\mathbf{c}}$. The examples described below assume acoustic sensors with a sound propagation speed of 342 ms^{-1} . For an aperture of 10 cm, one finds a useful frequency range (with condition number $< 150 \text{ dB}$) of at least 100–5000 Hz.

XI. EXAMPLES

Figure 3 shows the results obtained for a linear array of omnidirectional sensors with irregular spacing and an aperture of 10 cm. Arbitrary spacing of a small number of sensors ($N=3$ and $N=5$) was used to highlight the advantage of the present technique as compared to existing analytic methods, which typically require a larger number of sensors in a regular arrangement.

The figure shows that frequency invariance is reasonably well maintained up to the Nyquist frequency of 5000 Hz despite using only one set of coefficients (instead of separate coefficients for each of the $T/2+1$ frequency bins). Time

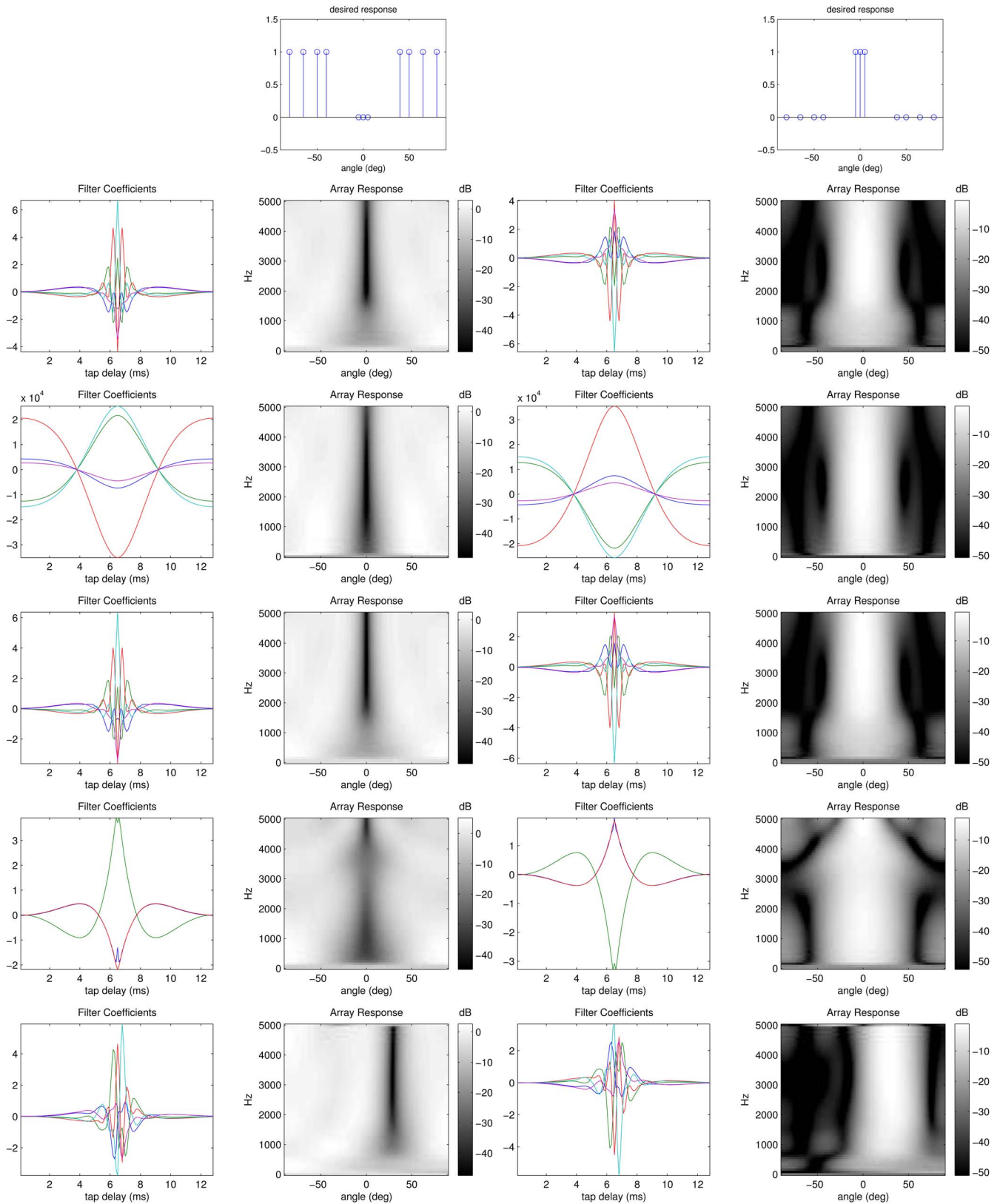


FIG. 3. (Color online) Frequency-invariant design of null beam (left) and main beam (right). Top panels show desired responses. Each following row compares results for different design parameters. First and third columns show time-domain filter coefficients $c_n(t)$. Second and third columns show magnitude response as function of frequency k and angle ϑ . Gray-scale represents response in dB. First row is obtained with a Legendre basis with five sensors assuming -30 dB noise. The same parameters are used for the following rows except that: Second row assumes zero noise; Third row uses naive basis; Fourth row uses only three microphones; Fifth row shifts the Legendre basis by 30° degrees.

domain coefficients were computed with $T=128$, which results in a reduction of the number of free parameters by a factor of 65.

In these examples, the Legendre basis included orders up to $L=20$, and the basis transform was computed with Eq. (33) using $Q=200$ equidistant samples ϑ_n . Compare this to

the third row showing the result with the naive basis. There is no significant difference to the Legendre basis (shown in the first row) despite the reduction of the number of parameters by a factor of $Q/L=10$. The Legendre basis therefore makes the array steerable and reduces the number of parameters without compromising accuracy. In practice, the order of the Legendre basis should be chosen depending on the desired angular bandwidth.

White noise with a power of -30 dB was assumed, except in the second row where no regularization was used, i.e., the basis was computed with Eq. (17). However, note that when the condition number exceeded 150 dB, those frequency bands were excluded regardless of the noise assumptions. Notice the significant scale increase in the filter coefficients indicating excessive low-frequency gain. Therefore, noise-based regularization should always be used in practice.

In these examples, $N=5$ sensors are located at $r_n=0, 2, 5, 7,$ and 10 cm. Compare this with the fourth row that has only $N=3$ sensors located at $r_n=0, 5,$ and 10 cm. This comparison indicates that the deviation from frequency invariance is primarily due to the limited number of sensors. Not surprisingly, as the number of sensors increases, frequency invariance is improved.

Finally, the last row demonstrates the effect of shifting the Legendre basis by an angle of $\beta=30^\circ$ (as in Fig. 2) leading to a corresponding shift of the beam pattern.

Simulations with different sensor locations (not shown) indicate that the performance of the proposed method does not depend significantly on the specific arrangement of sensors. This is expected as the proposed method is guaranteed to make the best use of a fixed and known sensor configuration. However, as with conventional beam-design methods, some sensor arrangements are better suited to minimize aliasing and increase resolution. The present work did not aim to determine such optimal sensor locations. See, for instance, Ref. 21 for a modern technique to optimize locations.

Similarly, the sensitivity to errors in sensor position is comparable to conventional beam design. Simulations on the examples above (not shown) indicate only minor effects for location errors of about 1 mm ($\approx 5\%$ of the microphone spacing) but a significant deterioration for larger position errors. As with conventional beam design, it is preferable to use adaptive rather than data-independent methods as they can adapt to position errors. Section IX outlined how to implement adaptive design methods using the frequency-invariant basis.

XII. CONCLUSION

The previous section demonstrated the proposed method on a linear array. The implementation for a volumetric array is straightforward using definition (4) or expansion (11) for \mathbf{G} , and using spherical harmonics (19) to define matrix $\tilde{\mathbf{G}}$ analogous to matrix \mathbf{P} . The linear array was chosen here because the resulting frequency-invariant beam patterns are easier to visualize on paper, and because steering required special consideration as a result of the restricted linear geometry. No such complication should arise for a volumetric array since the Wigner rotations in Eq. (18) are exact. For a

planar array, analogous considerations to those of the linear array may be necessary to cope with the symmetry across the array plane.

The presentation in this paper was restricted to omnidirectional sensors. However, the method applies equally well to sensors with directional response. If the sensor response is specified by $r(k, \Omega)$, then $g(k, \Omega)$ has to be replaced by $r(k, \Omega)g(k, \Omega)$ everywhere.

Finally, the notation here considers only the far-field response. One can generalize the argument to the near field by replacing plane waves of orientation Ω with point sources located at position \mathbf{r} . In that case, the array response to a planar wave, $g_n(k, \Omega)$, is to be replaced by the array response to a spherical wave,⁹ $g_n(k, \mathbf{r}) = e^{ik(\mathbf{r}-\mathbf{r}_n)} / \|\mathbf{r}-\mathbf{r}_n\|$, and \mathbf{r} has to be discretized over the desired range of point source positions when computing \mathbf{B} . The expansion for the spherical rather than a planar wave is given by Eq. (11) whereby the spherical Bessel function $j_l(kr'_n)$ is replaced by $j_l(kr'_n)/j_l(kr)$.⁹ The rationale leading to a steerable beam design remains fully applicable.

ACKNOWLEDGMENTS

This work was initially motivated by the work of Meyer and Elko on frequency-invariant spherical arrays,⁸ and the need to develop adaptive frequency-invariant beams for acoustic source separation.²² I would also like to thank Walter Kellermann for useful comments, Chris Alvino for his careful review of multiple versions of this manuscript, and the anonymous reviewers of an earlier conference paper²³ who highlighted the need to address the issue of noise and stability.

¹D. B. Ward, R. A. Kennedy, and R. C. Williamson, "Theory and design of broadband sensor arrays with frequency invariant far-field beam patterns," *J. Acoust. Soc. Am.* **97**, 1023–1034 (1995).

²T. Abhayapala, R. Kennedy, and R. Williamson, "Nearfield broadband array design using a radially invariant modal expansion," *J. Acoust. Soc. Am.* **107**, 392–403 (2000).

³R. Kennedy, T. Abhayapala, and D. Ward, "Broadband near-field beamforming using a radial beampattern transformation," *IEEE Trans. Signal Process.* **46**, 2147–2156 (1998).

⁴W. Liu and S. Weiss, "A new class of broadband arrays with frequency invariant beam patterns," in *Proceedings of the International Conference on Acoustics, Speech, and Signal Processing* (IEEE, New York, 2004), Vol. **2**, pp. 185–188.

⁵D. B. Ward, R. A. Kennedy, and R. C. Williamson, "FIR filter design for frequency invariant beamformers," *IEEE Signal Process. Lett.* **3**, 69–71 (1996).

⁶T. Sekiguchi and Y. Karasawa, "Wideband beamspace adaptive array utilizing FIR fan filters for multibeam forming," *IEEE Trans. Signal Process.* **48**, 277–284 (2000).

⁷H. Teutsch and W. Kellermann, "EB-ESPRIT: 2D Localization of multiple wideband acoustic sources using eigenbeams," in *Proceedings of the International Conference on Acoustics, Speech, and Signal Processing* (IEEE, New York, 2005), Vol. **3**, pp. 89–92.

⁸J. Meyer and G. Elko, "A highly scalable spherical microphone array based on an orthonormal decomposition of the soundfield," in *Proceedings of the International Conference on Acoustics, Speech, and Signal Processing* (IEEE, New York, 2002), Vol. **2**, pp. 1781–1784.

⁹E. G. Williams, *Fourier Acoustics* (Academic, New York, 1999).

¹⁰A. Edmonds, *Angular Momentum in Quantum Mechanics* (Princeton University Press, Princeton, N.J., 1957).

¹¹Z. Li and R. Duraiswami, "A robust and self-reconfigurable design of spherical microphone array for multi-resolution beamforming," in *Proceedings of the International Conference on Acoustics, Speech, and Signal*

Processing (IEEE, New York, 2005), Vol. 4, pp. 1137–1140.

- ¹²Z. Li and R. Duraiswami, “Hemispherical microphone arrays for sound capture and beamforming,” in *Proceedings of the Workshop on Applications of Signal Processing to Audio and Acoustics* (IEEE, New York, 2005), pp. 106–109.
- ¹³S. Chan and C. Pun, “On the design of digital broadband beamformer for uniform circular array with frequency invariant characteristics,” in *Proceedings of the International Symposium on Circuits and Systems* (IEEE, New York, 2002), Vol. 1, pp. 693–696.
- ¹⁴E. Wigner, *Gruppentheorie und ihre Anwendungen auf die Quantenmechanik der Atomspektren (Group theory and its applications to the quantum mechanics of atomic spectra)* (Friedr. Vieweg, and Sohn, Berlin, 1931).
- ¹⁵C. H. Choi, J. Ivanic, M. S. Gordon, and K. Ruedenberg, “Rapid and stable determination of rotation matrices between spherical harmonics by direct recursion,” *J. Chem. Phys.* **111**, 8825–8831 (1999).
- ¹⁶R. Jakob-Chien and B. K. Alpert, “A fast spherical filter with uniform resolution,” *J. Comput. Phys.* **136**, 213–230 (1997).
- ¹⁷R. Duraiswami, Z. Li, D. Zotkin, E. Grassi, and N. Gumerov, “Plane-wave decomposition analysis for spherical microphone arrays,” in *Proceedings of the Workshop on Applications of Signal Processing to Audio and Acoustics* (IEEE, New York, 2005), pp. 150–153.
- ¹⁸P. N. Swartztrauber, “The spectral approximation of discrete scalar and vector functions on the sphere,” *SIAM (Soc. Ind. Appl. Math.) J. Numer. Anal.* **16**, 934–949 (1979).
- ¹⁹P. N. Swartztrauber and W. F. Spitz, “Spherical harmonics projectors,” *Math. Comput.* **73**, 753–760 (2003).
- ²⁰B. Van Veen and K. Buckley, “Beamforming techniques for spatial filtering,” *Digital Signal Processing Handbook* (CRC Press, New York, 1997), pp. 61.1–61.20.
- ²¹S. Blank and M. Hutt, “On the empirical optimization of antenna arrays,” *IEEE Antennas Propag. Mag.* **47**, 58–67 (2005).
- ²²W. Liu and D. Mandic, “Semi-blind source separation for convolutive mixtures based on frequency-invariant transformation,” in *Proceedings of the International Conference on Acoustics, Speech, and Signal Processing* (IEEE, New York, 2005).
- ²³L. C. Parra, “Least squares frequency invariant beamforming,” in *Proceedings of the Workshop on Applications of Signal Processing to Acoustics and Audio* (IEEE, New York, 2005).